Articles in PresS. Am J Physiol Heart Circ Physiol (February 24, 2017). doi:10.1152/ajpheart.00685.2016

High-throughput screening identifies microRNAs that target Nox2 and improve function following acute myocardial infarction

Junyu Yang[1,2], Milton E. Brown[2], Hanshuo Zhang[1]; Mario Martinez[2]; Zhihua Zhao[1]; Srishti Bhutani[2], Shenyi Yin[1], David Trac[2], Jianzhong Jeff Xi[1,2,3,4], Michael E. Davis[1,2,5,*]

[1]Department of Biomedical Engineering, College of Engineering, Peking University, Beijing, China

[2]Wallace H. Coulter Department of Biomedical Engineering at Emory University and Georgia Institute of Technology, Atlanta, GA, USA

[3]State Key Laboratory of Natural and Biomimetic Drugs, Department of Biomedical Engineering, College of Engineering, Peking University, China

[4]State Key Laboratory of Biomembrane and Membrane Biotechnology, Institute of Molecular Medicine, Peking University, China

[5]Division of Cardiology, Department of Medicine, Emory University School of Medicine, Atlanta, GA, USA

*Corresponding authors:
Michael E. Davis, PhD
Associate Professor of Biomedical Engineering
Wallace H. Coulter Department of Biomedical Engineering at
Emory University and Georgia Institute of Technology
1760 Haygood Drive, Suite W200
Atlanta, GA 30322
michael.davis@bme.emory.edu

Running title: MicroRNAs targeting Nox2

Abstract

Aims: Myocardial infarction (MI) is the most common cause of heart failure. Excessive production of reactive oxygen species plays a key role in the pathogenesis of cardiac remodeling after MI. NADPH with Nox2 as the catalytic subunit is a major source of superoxide production and expression is significantly increased in the infarcted myocardium, especially by infiltrating macrophages. While microRNAs (miRNAs) are potent regulators of gene expression, and play an important role in heart disease, there still lacks efficient ways to identify miRNAs that target important pathological genes for treating MI. Thus, the overall objective was to establish a miRNA screening and delivery system for improving heart function after MI using Nox2 as a critical target.

Methods and Results: By utilizing the miRNA-target screening system comprised of a self-assembled cell microarray(SAMcell), three miRNAs, miR-106b, miR-148b, and miR-204, were identified that could regulate Nox2 expression and its downstream products both in human and mouse macrophages. Each of these miRNAs were encapsulated into polyketal (PK3) nanoparticles that could effectively deliver miRNAs into macrophages. Both in vitro and in vivo studies in mice confirmed the PK3-miRNAs particles could inhibit Nox2 expression and activity, and significantly improve infarct size and acute cardiac function after MI.

Conclusions: Our results show that miR-106b, miR-148b and miR-204 were able to improve heart function after myocardial infarction in mice by targeting Nox2 and possibly altering inflammatory cytokine production. This screening system and delivery method could have broader implication for miRNA-mediated therapeutics for cardiovascular and other diseases.

Keywords: microRNA; oxidative stress; myocardial infarction

New and noteworthy: Nox2 is a promising target for treating cardiovascular disease but there are no specific inhibitors. Finding endogenous signals that can target Nox2 and other inflammatory molecules is of great interest. In this study, we used high-throughput screening to identify microRNAs that target Nox2 and improve cardiac function following infarction.

Introduction

Myocardial infarction (MI) is the leading cause of heart failure (HF), which results in tremendous morbidity and mortality worldwide (10). MI leads to scar formation and adverse cardiac remodeling including changes in the molecular and structural components of the myocardium, which lead to cardiac dysfunction (1). Following MI, circulating blood monocytes respond to chemotactic factors, migrate into the infarcted myocardium, and differentiate into macrophages. In addition, neutrophils and other inflammatory cells migrate to the injured myocardium acutely and initiate a wound healing response (7). While studies show that low levels of reactive oxygen species (ROS) are physiologically important, production of excessive amounts of ROS is a key event involved in post-MI pathogenesis (8). ROS modulate several processes during cardiac remodeling, including interstitial fibrosis, and cardiomyocyte apoptosis and hypertrophy (4, 23).

Many studies demonstrate that a major source for ROS in the heart comes from a family of nicotinamide adenine dinucleotide phosphate- (NADPH) oxidase enzymes (5). NADPH oxidase is a multi-subunit enzyme consisting of membrane proteins ($gp91^{phox}$ otherwise known as Nox and $p22^{phox}$) and several intracellular associated proteins ($p47^{phox}$, $p67^{phox}$, Rac). Five Nox isoforms (Nox1 to Nox5) exist and are thought to the major indispensable subunit. Among these, Nox2 is expressed in cardiomyocytes, fibroblasts, and endothelial cells, and is thought to be dominant Nox isoform contributing to cardiac superoxide levels (O_2^-) production (2, 23). Evidence shows that both in animal models of MI and patients with end-stage heart failure, Nox2 expression is significantly increased in the infarcted myocardium, primarily in macrophages and myocytes (14, 19). Nox2 knockout mice show reduced cardiomyocyte apoptosis and adverse remodeling after MI and attenuate interstitial fibrosis following aortic constriction (12, 23). Recent studies show that Nox2 overexpression in cardiomyocytes does not alter infarct size, but rather long-term remodeling, indirectly demonstrating a role of inflammatory cell Nox2 in this process (27). In addition, as there is no specific inhibitor of Nox2, studies from our own laboratory have shown that Nox2 siRNA delivered in polymeric nanoparticles can attenuate acute cardiac dysfunction following MI as a potential therapeutic alternative (29).

MicroRNAs (miRNAs) are endogenous small noncoding RNAs, about 22 nucleotides in length, which can mediate post-transcriptional gene silencing by binding to the 3'-untranslated regions (3'UTR) of target mRNAs and inducing translational inhibition or RNA decay(18). miRNAs are involved in diverse biological progresses, including cellular differentiation, proliferation, apoptosis, and migration (15, 30, 37). miRNAs have been demonstrated as a significant regulation factor in cardiovascular diseases. For example, miR-24 has been shown to be upregulated after cardiac ischemia and its inhibition can prevent endothelial cell apoptosis and increase vascularity, which results in preservation of cardiac function and survival (9). Meanwhile, overexpression of miR-21 significantly decreased infarct size in mice after ischemia/reperfusion (IR) injury (25). Another study reportedmiR-34a to be up regulated after MI (34). Knockdown of miR-34a in mice could significantly improve hearts post-MI remodeling.

The critical challenge in miRNA therapy for cardiac disease includes identifying miRNAs that can target important genes and delivering them into specific cells efficiently. A certain miRNA normally has hundreds of targets, which is difficult to validate only by database prediction. Most published works using high-throughput miRNA target validation are used to identify targets of a miRNA (13, 24, 31). However, for a specific pathological disease, in which we already know which genes play important roles, it is more useful to find and select miRNAs that can target those genes directly. As Nox2 has no specific inhibitor and plays such an important role in post-MI pathogenesis, finding new ways to reduce expression could generate

new therapeutic options. Moreover, to date, there have been no reports of miRNAs that target Nox2 directly and reduce expression. In this study, we demonstrate use of a self-assembled cell microarray (SAMcell) to find miRNAs that target Nox2 and deliver them into myocardial macrophages via acid-degradable polymers previously shown to deliver siRNA in to macrophages (29). The SAMcell system had been demonstrated for its efficient and accurate miRNA targeting identification by our previous work (35). SAMcell assays using the 3'UTR of Nox2 identified many potential miRNAs that were then tested in reporter cells, as well as mouse and human macrophages. Validated miRNA were loaded within polyketal nanoparticles for macrophage targeting and delivered following acute MI.

Methods

Cell culture procedures

miRNA mimics were obtained from GenePharma and Sigma. 293T and Hela cells were cultured in high-glucose Dulbecco's Modified Eagle Medium (DMEM) containing 10% fetal bovine serum (FBS), 100 units/ml penicillin and 0.1 mg/ml streptomycin (P/S). RAW 264.7 and THP-1 cells were cultured RPMI 1640 containing same amounts of FBS and P/S as above. All cells were cultured under humidified conditions in 5% CO_2 at 37°C. When seeding, cells were washed with PBS and incubated in 0.25% trypsin containing 5mmol/L EDTA. After centrifugation, cells were diluted in media, counted via hemocytometer, and then seeded at the appropriate concentration.

To achieve transient expression, plasmids and miRNA mimics were transfected using Oligofectamine (Invitrogen). The cell number and nucleotide were determined per manufacturer's protocol. To establish stable cell lines, the indicated lentiviral vectors were packaged and transfected into cells. In brief, lentivirus was packaged into 293T cells, and then harvested and infected to Hela cells. After 72 hours, cells were selected and collected by FACS.

Luciferase assays

For luciferase assays, the 3'UTR of human or mouse Nox2 were cloned into pGL3 plasmids 3' to the firefly luciferase gene. Four x 10^4 293T cells were co-transfected with 200 ng of the indicated pGL3 firefly luciferase construct and 20 ng of a pGL3 Renilla luciferase used as a normalization control. At the same time, the indicated miRNA expression plasmid or mimics were transfected. After 48 hours, cells were lysed and luciferase activities were measured using the Dual Luciferase Reporter Assay System (Promega).

Screening of miRNA-targets using self-assembled cell microarray (SAMcell)

The fabrication of the SAMCell microarray had been previously described (36). In brief, the glass slides (22 mm x 22 mm) were covered with Poly (N-isopropylacrylamide) (Aldrich) dissolved in ethanol (6% w/v). The slides were etched via a shadow mask by oxygen plasma for 3.5 min at 200w power. The reverse transfection protocol described below refers to a previous description (36). The miRNA mimic library mixed in the reverse transfection reagent was printed on the chip (Suzhou Genoarray Co., Ltd.) Next, the slides were fixed in a 6-well plate by melted wax. A reporter system was built that expresses an enhanced green fluorescent protein (eGFP). Then the 3'UTR of human Nox2 was cloned as the 3'UTR of eGFP and a stable Hela cell line expressing the reporter system was selected by FACS as described above. Over 260 miRNAs were printed on the SAMcell chip. Then, 5 x 10^5 cells containing 3'UTR reporter were transferred into each well. After culturing for 48 hours, the dishes were moved to room temperature for 5 min and washed with PBS for three times to remove the polymer. Average fluorescent intensity of each cell island were collected and analyzed. The cut-off value was obtained on the basis of the Kolmogorov-Smirnov Z-test in 50 control experiments. Six replicates were repeated for each miRNA.

Polyketal (PK3) synthesis

PK3 was synthesized as described in our prior study (20). Briefly, the diols, cyclohexanedimethanol and 1,5-pentanediol were dissolved in distilled benzene and heated to 100°C. Recrystallized p-toluenesulfonic acid (PTSA) was dissolved (~1 mg) in ethyl acetate and added to the benzene solution to catalyze the reaction. The polymerization reaction was initiated by the addition of equimolar 2,2-diethoxypropane (DEP). Additional 2,2-dimethoxy propane (DMP) and benzene were subsequently added to the reaction to compensate for loss of volume in the form of ethanol/methanol and the solvent benzene that had distilled off. After 48h, the reaction was stopped with triethylamine and isolated by precipitation in cold hexanes. The solid polymer was filtered off, rinsed in hexanes and vacuum dried prior to storage at -20°C. Polymer molecular weight/polydispersity was confirmed by gel permeation chromatography.

Preparation of miRNA-loaded PK3 particles

PK3-miRNA particles were prepared following the protocol for PK3-siRNA particles(29). Briefly,1mg miRNA in water and 2.2 mg of cationic lipid N-[1-(2,3-Dioleoyloxy)propyl]-N,N,Ntrimethylammonium methysulfate (DOTAP) dissolved in dichloromethane (DCM) were brought to one phase by addition of 1.05 mL of methanol. After 15 min incubation, an additional 0.5 mL of water and DCM were added and the mixture was vortexed, and centrifuged at 750 rpm for 5 min. The miRNA:DOTAP complex in the bottom organic layer was encapsulated in PK3 via an oil/water single emulsion procedure, using DCM as the oil phase and polyvinyl alcohol (PVA) as the surfactant stabilizer. 1 mL of DCM containing ion-paired miRNA was added to 40 mg of PK3 with 1 mg of chloroquine free base. This solution was homogenized into 8 mL of 5% (w/v) PVA solution at the highest setting in the Power Gen 500 (Fisher Scientific) for 30 seconds, and sonicated at an intermediate speed (Sonic dismembrator model 100, Fisher Scientific) with 10 pulses of 1 sec duration. The emulsion was then dispersed in a 20 mL of 0.5% PVA solution and stirred for a period of 4-5 h to allow the DCM to evaporate. The resulting particles were isolated by centrifugation (15000 rpm, 20 min), washed three times, freeze-dried and stored at -20°C for further use.

In vitro delivery of PK3-miRNA particles

For in vitro studies, RAW 264.7 macrophages or PMA induced THP-1 cells were plated in 6-well plates at a density of 1 x 10^6cells per well. After 24 h, cells were treated with indicated PK3-miRNA particles at a concentration of particles equivalent to 2 µg miRNA/well. For gene expression studies, following 48 hours of treatment, the cells were harvested and RNA or protein extracted. For assessment of functional activity of Nox2-NADPH, the cells were kept in wells for analysis of O_2^- production.

Gene expression by real-time PCR and western blot

Total RNA from cells was isolated using Trizol (Invitrogen) according to the manufacturer's protocol. Complementary DNA (cDNA) was synthesized using SuperScript III kit (Invitrogen). Real time PCR was performed using Power SYBR Green (Invitrogen) master mix with Applied Biosystems StepOne Plus real time PCR system. The primers used are listed in Supplementary Table 1. Nox2 gene expression levels were normalized to the housekeeping gene GAPDH. Total protein extracted from cells were resolved by SDS-PAGE and then transferred to a polyvinylidene difluoride membrane (Millipore Corporation). The membranes were probed with antibodies against Nox2 (Abcam) and GAPDH (Abcam). The images were obtained and quantified by Image J software.

Supernatant Collection and Enzyme-Linked Immunosorbent Assay

Forty-eight hours after transfection with indicated miRNAs, Raw246.7 media were collected for

analysis. The concentrations of IL-1β, IL-6, and TNF-α in the supernatant were determined by enzyme-linked immunosorbent assay (R&D Systems). All assays were performed according to the manufacturer's protocol.

Detection of superoxide in vitro and in vivo

To test Nox2 activity in vitro, production of O_2^- after stimulation with phorbol-12-myristate 13-acetate (PMA) was measured by staining with fluorescent ROSstar 650 dye. Forty-eight hours after transfection with miRNAs or treatment with PK3-miRNA particles, media was aspirated from wells containing induced THP-1 or RAW 264.7 macrophages and then washed with fresh cold Krebs-Hepes buffer (KHB). Then 10 μM PMA was added to each well and incubated for 10 min at 37°C. After this, 25 μM dye was added to wells and incubated for 20 minutes under dark conditions. For in vivo studies, frozen sections were washed by KHB and stained with dihydroethidium (DHE) directly for 20 minutes. Fluorescent images were taken by Nikon fluorescent microscope using equal exposure times for all samples.

Myocardial infarction and particle injection

Studies were conducted under a randomized and blinded manner. Adult male C57BL/6 mice (>8 weeks) were used and assigned to five groups. One group was subjected to sham surgery, while the other four groups received permanent myocardial infarction. The surgeries were conducted as described previously (26). Briefly, the animals were anesthetized by isoflurane (1-3% inhaled). Following tracheal intubation, the heart was exposed by separation of the ribs. Myocardial infarction was achieved by ligation of the left anterior descending coronary artery. For mice getting particle injections, 50 μL of indicated particle was injected into the cyanotic ischemic zone through a 30-gauge needle immediately after ligation. The dose of miRNA injected was 5 μg/kg. After injection, the chests were closed and animals were recovered on a heating pad. Animals were euthanized by regulated carbon dioxide inhalation in a closed chamber per proper guidelines. Functional assessments were made at 3 days following surgeries using echocardiography. These studies conformed to the Guide for the Care and Use of Laboratory Animals published by the US National Institutes of Health and all animals studies were approved by Emory University Institutional Animal Care and Use Committee.

Immunohistochemistry

Fresh heart tissue was frozen in Tissue-Tek OCT and 5μm sections were made. After washing with PBS, sections were fixed by 4% formaldehyde solution an then incubated with goat serum for 1 h. Nox2 antibody diluted in goat serum was added to the sections and incubated at 4°C overnight. After that, sections were washed 3 times using PBS-Tween and incubated with fluorescent secondary antibody for 2 h at room temperature. At least 3 sections from each animal were analyzed. Nuclei were stained by Hoechst dye. Images were taken by Nikon at identical exposures and analyzed by ImageJ software.

Echocardiography and infarct size

Anesthetized mice were subjected to echocardiography 3 days after MI surgery. Short axis values of left ventricular diameter were obtained using a Vevo 770 small animal ultrasound system (Visualsonics). An average of 3 consecutive cardiac cycles was used for each measurement and performed three times in an investigator-blinded manner. Fractional shortening (FS) was calculated as (end-diastolic diameter - end-systolic diameter)/end-diastolic diameter and expressed as a percentage.

Myocardial infarct size was evaluated using 2,3,5-triphenyltetrazolium chloride (TTC) staining and Evans Blue dye in which the percent area of infarction was calculated as the infarcted area (TTC stained) divided by the ischemic area at risk at 24 hours following injury.

Statistics

For statistical analysis, two-sided Student t tests were used for in vitro studies, while one-way ANOVA tests were used for in vivo studies. A p-value < 0.05 was considered statistically significant. * P < 0.05; ** P < 0.01; *** P < 0.001. Error bars indicate SD of at least three independent experiments.

Results

SAMCell screening to target human Nox2

The schematic diagram of screening system is shown as **Figure 1**. The 3'UTR of human Nox2 was cloned into reporter system and266 miRNAs, conserved between human and mouse, were screened by SAMCell assay. The top effective miRNAs are listed in Table 1. Three miRNAs, miR-106, miR-148b, and miR-204 were selected for further study after literature research and miRNA target prediction. Each of them have one or more predicted binding sites in human Nox2 3'UTR according to Targetscan database, shown in Table 2.

Selected miRNAs functional validation

To validate each miRNA's ability to suppress human Nox2, we performed luciferase assaysin 293T cells cloned with the 3'UTR of Nox2 downstream of luciferase. As shown in **Figure 2A**, all of the three miRNAs significantly decreased luciferase expression compared to control (miR-106b=78.5$\pm$8.6%, P<0.01; miR-148b=78.6$\pm$11.1%, P<0.01; miR-204=56.2$\pm$8.4%, P<0.001).Additionally, we mutated the predicted binding sites in the 3'-UTR and found no effect of the selected miRNAs. To determine whether their regulation was conserved, we also validated the selected miRNAs using mouse Nox2 3'UTR downstream of luciferase. Similar to human Nox2, luciferase containing mouse Nox2 3'UTR was also significantly decreased by these miRNAs compared to control group (miR-106b=66,6$\pm$6.8%, P<0.001; miR-148b=70.1$\pm$8.2%, P<0.001; miR-204=46.7$\pm$2.7%, P<0.001, **Figure 2B**).

We also transfected these miRNAs mimics to induced human macrophages (THP-1 cells) and a mouse macrophage cell line (RAW 264.7). Nox2 mRNA and protein levels were detected by real-time PCR and western blot, respectively. As expected, compared to a scrambled control miRNA group, all 3 miRNAs decreased both human and mouse Nox2 expression at the gene and protein level by about 40% (**Figure 2C and 2D**).

In vitro functional knockdown of Nox2 downstream production

To determine whether Nox2 knockdown by miRNAs resulted in functional changes, we transfected THP-1 induced and RAW 264.7 macrophages with miRNAs separately and 48 hours later, they were stimulated with PMA to induce O_2^- production. ROSstar 650 dye, a fluorescent probe for intracellular ROS, was then added to the cells. Fluorescence intensity was expressed as fold change in O_2^- production normalized to basal O_2^- levels. As shown in **Figure 3A**, after stimulation with PMA, O_2^- production was increased, while each miRNA treatment groupshowed significantly decreased levels in O_2^- production compared to the control group in THP-1 induced (upper) and RAW 264.7 (bottom) macrophages. Quantification results were shown as **Figure 3B** for THP-1 induced macrophages and **Figure 3C** for RAW 264.7 macrophages. In order to investigate if the inhibition of O_2^- production was a result of decreased Nox2, we overexpressed Nox2 protein concurrently with miRNAs transfection. As shown in **Figure 3D-E,** O_2^- production level was partially rescued when Nox2 was overexpressed.

We also examined whether the miRNA identified were additive, and whether there were effects on other inflammatory targets. There was no significant additive effect by delivery of all three miRNAs together compared to the single miRNA alone both for Nox2 expression level and O_2^- production level (**Figure 4A and 4B**). We also investigated expression of IL-1α, IL-6 and

TNF-α by real-time PCR in RAW 264.7 macrophages after transfection with miRNAs. As **Figure 4C-E** show, these miRNAs significantly decreased the mRNA expression level of these pro-inflammatory genes as well, except miR-148b on TNF-α. To further identify miRNAs' effects on the protein level of these three genes, enzyme-linked immunosorbent assay was used and the expression of secreted proteins were all inhibited when any miRNA was overexpressed, as shown in **Figure 4F-H**.

Nanoparticle uptake by macrophages

After validation of individual miRNA function on Nox2 expression and downstream O_2^- production, we sought to validate our previously used in vivo delivery system with miRNA in cultured cells. miRNAs encapsulated within PK3 polymer(PK-miRNA)showed similar loading levels as our prior publications (1 μg per mg particle). Cells were incubated with the indicated PK-miRNA formulation and expression of the delivered miRNA was evaluated with real-time PCR. As shown in in **Figure 5A**, each formulation was able to increase expression of their respective cargo at least 500-fold, indicating effective delivery.

We treated RAW 264.7 macrophages with PK-miRNA particles for 48 hours and Nox2 mRNA expression level was determined by real-time PCR. As shown in **Figure 5B**, treatment with any of the particle formulations significantly reduced Nox2 gene expression (miR-106b=58.9$\pm$5.7%, P<0.001; miR-148b=63.7$\pm$7.9%, P<0.001; miR-204=51.1$\pm$12.8%, P<0.001). O_2^- production was also measured and, similarly to gene expression, treatment with any PK-miRNA particle significantly decreased production as compared to the control group (PK3-NC, **Figure 5C and 5D**).

PK-miRNAs delivery in vivo

To determine the in vivo efficiency of miRNA mediated-Nox2 suppression, adult male C57BL/6 mice were randomized into 5 treatment groups. Control mice were subjected to sham surgery, while the other four groups received MI surgery followed by injection of PK-miRNA or a negative control scrambled miRNA particle (PK-NC). At 3-days post injury, hearts were harvested and expression of Nox2 was determined by immunofluorescence staining of frozen sections. As shown in **Figure 6A and 6B**, there was a significant increase in Nox2 staining with PK-NC treatment following MI as compared to sham mice (about 3-fold, P<0.001). Compared to PK-NC group, each PK-miRNA treatment group demonstrated significantly reduced staining of Nox2(miR-106b=43.2$\pm$6.8%, P<0.001; miR-148b=24.8$\pm$6.3%, P<0.001; miR-204=35.9$\pm$5.1%, P<0.001). Additionally, O_2^-levels were determined by DHE staining on frozen sections. Similar to Nox2 expression levels, each PK-miRNA treatment significantly reduced the elevated DHE staining at least 50% (**Figure 6C and 6D**).To further identify if Nox2 was specifically inhibited in macrophages, we stained sections for Nox2 and CD68. As shown in **Figure 6E**, there was decreased co-staining in PK-miRNA treatment group, compared to PK-NC group.

To determine the effect of PK-miRNAs delivery on acute cardiac function after MI, echocardiography data was collected 3 days after injury. As shown in **Figure 7A, 7B and 7C**, MI significantly reduced cardiac function as measured in absolute change in fractional shortening and ejection fraction 3 days post-injury. Treatment with each PK-miRNA particle significantly improved function, restoring it to sham levels. To further examine functional changes, we also measured infarct size at 24 hours by TTC staining. As the representative images and grouped data show, each PK-miRNA particle significantly inhibited infarct size.

Discussion

Substantial evidence shows that oxidative stress due to excessive ROS such as O_2^- plays an important role in the development of post-MI cardiac dysfunction (8, 23). Antioxidant treatment following MI in animal models improves cardiomyocyte survival, attenuates ventricular

remodeling, and results in preservation of left ventricular function (4). NAPDH oxidases are major sources of O_2^- in the heart andthe family of gp91 proteins (Nox 1-5) is an important catalytic unit of the NADPH oxidase (23). Nox2 is mainly expressed in macrophages, fibroblasts, endothelial cells and cardiomyocytes (2) and is significantly increased in the myocardium following MI with the massive influx of inflammatory cells (14, 19). Nox2 is also increased in human cardiomyocytes following MI (14). Nox2 knockout mice are protected from post-MI dysfunction (12, 23), and studies from our own laboratory show that siRNA against Nox2 encapsulated in nanoparticles can protect against acute MI dysfunction (29). Therefore finding additional way to target Nox2 could be a promising therapeutic approach for preserving function following acute MI.

In the current report, we successfully identified several miRNAs targeting Nox2 with the use of a high-throughput miRNA-target screening system and validated their targeting using a luciferase reporter system with the 3'UTR of Nox2. We also confirmed their function by testing Nox2 expression and function in both human and mouse macrophage cell lines. To date, there had been no studies that identified a miRNA that directly bound the Nox2 3'UTR and decreased expression. The SAMcell assay provided a straightforward way to identify miRNAs that target a specific gene. In our previous studies, the performance of this system had been demonstrated using a phenotypic approach to determine miRNAs that regulated processes involved in cancer (35). In this study, miRNAs were selected that were conserved between human and mouse in order to test potential human targets in mouse models of MI. Three specific miRNAs were chosen for more detailed analysis due to prior publications underscoring their involvement in post-MI healing. Following MI, miR-106b reduced apoptosis via inhibition of p21 expression (22), and has also been shown to target the pro-inflammatory cytokine IL-8 (6). The second hit, miR-148b, has been reported to negatively regulate LPS-induced cytokine production in dendritic cells, including IL-6, IL-12, and TNF-α, and plays an important role in immune regulation (21). In addition, a significantly decreased expression of miR-148b was observed in isoproterenol-induced myocardial injury and fibrosis; expression was increased when apocynin treatment was used to reverse this (33). Finally, our third hit, miR-204, was decreased after ischemia-reperfusion (IR) injury in mice and overexpression of miR-204 protected the cardiomyocytes against IR-induced autophagy (32).

After selection of these three miRNAs, their inhibition of both human and mouse Nox2 was validated by several methods. Luciferase assays using the Nox2 3'UTR demonstrated they could each decrease Nox2 expression directly by canonical miRNA regulation. Real-time PCR and western blot studies confirmed that all three miRNAs decreased Nox2 levels at the gene and protein levels (Figure 2C-F).DHE staining for PMA-induced superoxide levels (a surrogate of Nox2 activity) also showed the functional benefit of the miRNA-induced decrease in Nox2 levels.

Once miRNAs were selected and validated, we sought to utilize an efficient delivery system for targeting macrophages in vivo. Polyketals are a class of delivery vehicles formulated from a class of polymers that contain pH-sensitive, hydrolyzable ketal linkages in their backbone. We had used the polyketal PK3 to deliver miRNA to bone marrow mononuclear cells to induce pluripotency (28). There was no difference in miRNA transfection efficiency between commercial transfection reagent (Oligofactamine) and PK3 nanoparticles (data not shown). Additional published studies from our laboratory demonstrated that PK3 nanoparticles were retained in the myocardium after injection and could be used to deliver siRNA following MI in mice (29). When engaged by macrophages, particles were taken up into phagosome/endosomes where they degrade due to the acidic environment, leading to release of cargo into the cytoplasm of macrophages (over 80% transfection efficiency). In that study we successfully delivered Nox2

siRNA into cardiac macrophages by PK3 particles and observed a significant improvement in heart function after MI.

Despite our prior study showing beneficial effects of delivery of siRNA to Nox2, delivery of miRNA might have potential advantages. Firstly, miRNA is more natural as there is no siRNA in mammalian cells. miRNA is viewed as endogenous and purposefully expressed products in an organism's own genome, whereas siRNA is thought to be primarily exogenous in origin, derived directly from viruses, transposons, or transgene triggers (3). Additionally, introduction of too much siRNA could result in nonspecific events due to activation of innate immune response (17). Secondly, miRNA could target many genes and sometimes from the same pathways. For example, let-7, which was shown to be able to directly regulate some key cell cycle proto-oncogenes, e.g., RAS, CDC25a, CDK6, and cyclin D at the same time, was a key regulator of cell proliferation (16). Likewise, miR-23b plays an important role in tumor metastasis since it regulates a cohort of pro-metastatic targets, including FZD7, MAP3K1, TGFBR2 and PAK2 (36). To validate this hypothesis in this study, we examined expression levels of other pro-inflammatory genes such as IL-1α, IL-6 and TNF-α by real-time PCR and ELISA assay in RAW 264.7 cytokines after transfection with miRNAs and found that all miRNAs also targeted other inflammatory genes, though it is unclear as to whether this was indirect or direct.

We next examined the efficacy of these particles in vivo, in a mouse model of MI. Similar to our prior studies, we delivered particles immediately following ligation to the border zone of the infarct. In keeping with published studies (12, 14, 19), both Nox2 levels and superoxide levels were significantly increased following MI. While Nox2 levels have been shown to be upregulated in cardiomyocytes, staining indicated upregulation in both cardiomyocyte and non-cardiomyocyte origin, likely infiltrating inflammatory cells. Double staining indicated that CD68-positive macrophages had expression of Nox2 that was not present in any PK-miRNA treated groups. While we did not identify the source of the superoxide, it was also likely inflammatory cells based on prior studies (4, 23). While it is possible that Nox2 was increased in myocytes, our published studies show that polyketals are not efficiently taken up by cardiomyocytes without surface modification of the nanoparticles (11, 20). Thus, any reduction in Nox2 in cardiomyocytes was likely indirect, possibly an effect of reduced local superoxide and inflammation. It would be interesting to encapsulate the miRNAs in modified particles and determine whether miRNA-mediated knockdown of Nox2 in cardiomyocytes is sufficient for protection, though this would be unlikely due to the large influx of inflammatory cells. Additionally, we did not measure other ROS such as hydrogen peroxide (H_2O_2), which could also mediate damage. The role of H_2O_2 in acute MI is controversial and it remains a debate as to whether this is a valid target as H_2O_2 is also involved in important physiological processes. It is also likely that reduced levels of O_2^- also resulted in decreases in H_2O_2 and understanding this balance could be an interesting topic for future consideration. After treatment with any PK3-miRNA, Nox2 expression and O_2^-levelswere reduced significantly compared to the empty particle group. More importantly, an improvement in cardiac function and reduction in infarct size were observed in each PK3-miRNA formulation treatment group. These results corroborated reports that knockdown of Nox2 improves cardiac function after MI.

In conclusion, we have found novel miRNA regulation of Nox2 expression by utilizing a high throughput miRNA-target screening method, the SAMcell assay, to narrow down potential targets, specifically miR-106b, 148b, and 204. We validated the results in transfected cells, as well as human and mouse macrophages. Combined with our efficient macrophage-specific delivery approach, these miRNAs were able to reduce Nox2 expression and activity in vivo, resulting in improved acute function. With the robust nature of these systems, other inflammatory molecules can be studied to determine optimal miRNA candidates to modulate

inflammation in vivo.

Acknowledgments

The authors acknowledge the support of the Emory/GT/PKU program, as well as a Chinese Scholarship Council Fellowship to JY. This work was also supported by HL090601 to MED and NSFC grant numbers 81325010, 81421004 and 31371443.

Disclosures

None

References

1. **Anversa, P., P. Li, X. Zhang, G. Olivetti and J. M. Capasso.** Ischaemic myocardial injury and ventricular remodelling. *CardiovascRes*. 1993; **27**(2): 145-157.
2. **Bendall, J. K., A. C. Cave, C. Heymes, N. Gall and A. M. Shah.** Pivotal role of a gp91(phox)-containing NADPH oxidase in angiotensin II-induced cardiac hypertrophy in mice. *Circulation*. 2002; **105**(3): 293-296.
3. **Carthew, R. W. and E. J. Sontheimer.** Origins and Mechanisms of miRNAs and siRNAs. *Cell*. 2009; **136**(4): 642-655.
4. **Cave, A.**Selective targeting of NADPH oxidase for cardiovascular protection. *Curr OpinPharmacol*. 2009;**9**(2): 208-213.
5. **Cave, A. C., A. C. Brewer, A. Narayanapanicker, R. Ray, D. J. Grieve, S. Walker and A. M. Shah.** NADPH oxidases in cardiovascular health and disease. *Antioxid Redox Signal*. 2006; **8**(5-6): 691-728.
6. **Chuang, T. D., X. Luo, H. Panda and N. Chegini.** miR-93/106b and their host gene, MCM7, are differentially expressed in leiomyomas and functionally target F3 and IL-8. *Mol Endocrinol*. 2012;**26**(6): 1028-1042.
7. **Ertl, G. and S. Frantz.** Healing after myocardial infarction. *Cardiovasc Res*. 2005; **66**(1): 22-32.
8. **Ferdinandy, P. and R. Schulz.** Nitric oxide, superoxide, and peroxynitrite in myocardial ischaemia-reperfusion injury and preconditioning. *Br J Pharmacol*. 2003; **138**(4): 532-543.
9. **Fiedler, J., V. Jazbutyte, B. C. Kirchmaier, S. K. Gupta, J. Lorenzen, D. Hartmann, P. Galuppo, S. Kneitz, J. T. Pena, C. Sohn-Lee, X. Loyer, J. Soutschek, T. Brand, T. Tuschl, J. Heineke, U. Martin, S. Schulte-Merker, G. Ertl, S. Engelhardt, J. Bauersachs and T. Thum.** MicroRNA-24 regulates vascularity after myocardial infarction. *Circulation*. 2011; **124**(6): 720-730.
10. **Go, A. S., et al.** Heart disease and stroke statistics--2013 update: a report from the American Heart Association. *Circulation*. 2013; **127**(1): e6-e245.
11. **Gray, W. D., P. Che, M. Brown, X. Ning, N. Murthy and M. E. Davis.** N-acetylglucosamine conjugated to nanoparticles enhances myocyte uptake and improves delivery of a small molecule p38 inhibitor for post-infarct healing. *J Cardiovasc Transl Res*. 2011; **4**(5): 631-643.
12. **Grieve, D. J., J. A. Byrne, A. Siva, J. Layland, S. Johar, A. C. Cave and A. M. Shah.** Involvement of the nicotinamide adenosine dinucleotide phosphate oxidase isoform Nox2 in cardiac contractile dysfunction occurring in response to pressure overload. *J Am Coll Cardiol*. 2006; **47**(4): 817-826.
13. **Hafner, M., M. Landthaler, L. Burger, M. Khorshid, J. Hausser, P. Berninger, A. Rothballer, M. Ascano, Jr., A. C. Jungkamp, M. Munschauer, A. Ulrich, G. S. Wardle, S. Dewell, M. Zavolan and T. Tuschl.** Transcriptome-wide identification of RNA-binding protein and microRNA target sites by PAR-CLIP. *Cell*. 2010;**141**(1): 129-141.
14. **Heymes, C., J. K. Bendall, P. Ratajczak, A. C. Cave, J. L. Samuel, G. Hasenfuss and A. M. Shah.** Increased myocardial NADPH oxidase activity in human heart failure. *J Am Coll Cardiol*. 2003;**41**(12): 2164-2171.
15. **Johnnidis, J. B., M. H. Harris, R. T. Wheeler, S. Stehling-Sun, M. H. Lam, O. Kirak, T. R. Brummelkamp, M. D. Fleming and F. D. Camargo.** Regulation of progenitor cell proliferation and granulocyte function by microRNA-223. *Nature*. 2008; **451**(7182): 1125-1129.
16. **Johnson, C. D., A. Esquela-Kerscher, G. Stefani, M. Byrom, K. Kelnar, D. Ovcharenko, M. Wilson, X. Wang, J. Shelton, J. Shingara, L. Chin, D. Brown and F. J. Slack.** The let-

7 microRNA represses cell proliferation pathways in human cells. *Cancer Res*. 2007; **67**(16): 7713-7722.
17. **Judge, A. D., V. Sood, J. R. Shaw, D. Fang, K. McClintock and I. MacLachlan.** Sequence-dependent stimulation of the mammalian innate immune response by synthetic siRNA. *Nat Biotechnol*. 2005;**23**(4): 457-462.
18. **Kim, V. N., J. Han and M. C. Siomi.** Biogenesis of small RNAs in animals. *Nat Rev Mol Cell Bio*l. 2009;**10**(2): 126-139.
19. **Krijnen, P. A., C. Meischl, C. E. Hack, C. J. Meijer, C. A. Visser, D. Roos and H. W. Niessen.** Increased Nox2 expression in human cardiomyocytes after acute myocardial infarction. *J Clin Pathol*. 2003;**56**(3): 194-199.
20. **Lee, S., S. C. Yang, C. Y. Kao, R. H. Pierce and N. Murthy.** Solid polymeric microparticles enhance the delivery of siRNA to macrophages in vivo. *Nucleic Acids Res*. 2009; **37**(22): e145.
21. **Liu, X., Z. Zhan, L. Xu, F. Ma, D. Li, Z. Guo, N. Li and X. Cao.** MicroRNA-148/152 impair innate response and antigen presentation of TLR-triggered dendritic cells by targeting CaMKIIalpha. *J Immunol*. 2010;**185**(12): 7244-7251.
22. **Liu, Z., D. Yang, P. Xie, G. Ren, G. Sun, X. Zeng and X. Sun.** MiR-106b and MiR-15b modulate apoptosis and angiogenesis in myocardial infarction. *Cell Physiol Biochem*. 2012; **29**(5-6): 851-862.
23. **Looi, Y. H., D. J. Grieve, A. Siva, S. J. Walker, N. Anilkumar, A. C. Cave, M. Marber, M. J. Monaghan and A. M. Shah.** Involvement of Nox2 NADPH oxidase in adverse cardiac remodeling after myocardial infarction. *Hypertension*. 2008; **51**(2): 319-325.
24. **Orom, U. A. and A. H. Lund.** Experimental identification of microRNA targets. *Gene*. 2010; **451**(1-2): 1-5.
25. **Roy, S., S. Khanna, S. R. Hussain, S. Biswas, A. Azad, C. Rink, S. Gnyawali, S. Shilo, G. J. Nuovo and C. K. Sen.** MicroRNA expression in response to murine myocardial infarction: miR-21 regulates fibroblast metalloprotease-2 via phosphatase and tensin homologue. *Cardiovasc Res*. 2009; **82**(1): 21-29.
26. **Seshadri, G., J. C. Sy, M. Brown, S. Dikalov, S. C. Yang, N. Murthy and M. E. Davis.** The delivery of superoxide dismutase encapsulated in polyketal microparticles to rat myocardium and protection from myocardial ischemia-reperfusion injury. *Biomaterials*. 2010; **31**(6): 1372-1379.
27. **Sirker A, Murdoch CE, Protti A, Sawyer GJ, Santos CX, Martin D, Zhang X, Brewer AC, Zhang M, Shah AM.** Cell-specific effects of Nox2 on the acute and chronic response to myocardial infarction. J Mol Cell Cardiol. 2016 Sep; 98:11-7.
28. **Sohn, Y. D., I. Somasuntharam, P. L. Che, R. Jayswal, N. Murthy, M. E. Davis and Y. S. Yoon.** Induction of pluripotency in bone marrow mononuclear cells via polyketal nanoparticle-mediated delivery of mature microRNAs. *Biomaterials*. 2013;**34**(17): 4235-4241.
29. **Somasuntharam, I., A. V. Boopathy, R. S. Khan, M. D. Martinez, M. E. Brown, N. Murthy and M. E. Davis.** Delivery of Nox2-NADPH oxidase siRNA with polyketal nanoparticles for improving cardiac function following myocardial infarction. *Biomaterials*. 2013; **34**(31): 7790-7798.
30. **Tay, Y., J. Zhang, A. M. Thomson, B. Lim and I. Rigoutsos.** MicroRNAs to Nanog, Oct4 and Sox2 coding regions modulate embryonic stem cell differentiation. *Nature*. 2008;**455**(7216): 1124-1128.
31. **Thomson, D. W., C. P. Bracken and G. J. Goodall.** Experimental strategies for microRNA target identification. *Nucleic Acids Res*. 2011;**39**(16): 6845-6853.
32. **Xiao, J., X. Zhu, B. He, Y. Zhang, B. Kang, Z. Wang and X. Ni.** MiR-204 regulates cardiomyocyte autophagy induced by ischemia-reperfusion through LC3-II. *J Biomed Sci*. 2011;**18**: 35.

33. **Yang, Q., J. Cui, P. Wang, X. Du, W. Wang, T. Zhang and Y. Chen.** Changes in interconnected pathways implicating microRNAs are associated with the activity of apocynin in attenuating myocardial fibrogenesis. *Eur J Pharmacol*. 2016; **784**: 22-32.
34. **Yang, Y., H. W. Cheng, Y. Qiu, D. Dupee, M. Noonan, Y. D. Lin, S. Fisch, K. Unno, K. I. Sereti and R. Liao.**MicroRNA-34a Plays a Key Role in Cardiac Repair and Regeneration Following Myocardial Infarction. Circ Res. 2015;**117**(5): 450-459.
35. **Yin, S., Y. Fan, H. Zhang, Z. Zhao, Y. Hao, J. Li, C. Sun, J. Yang, Z. Yang, X. Yang, J. Lu and J. J. Xi.** Differential TGFbeta pathway targeting by miR-122 in humans and mice affects liver cancer metastasis. *Nat Commun*. 2016;**7**: 11012.
36. **Zhang, H., Y. Hao, J. Yang, Y. Zhou, J. Li, S. Yin, C. Sun, M. Ma, Y. Huang and J. J. Xi.** Genome-wide functional screening of miR-23b as a pleiotropic modulator suppressing cancer metastasis. *Nat Commun*. 2011; **2**: 554.
37. **Zhang, Y., D. Liu, X. Chen, J. Li, L. Li, Z. Bian, F. Sun, J. Lu, Y. Yin, X. Cai, Q. Sun, K. Wang, Y. Ba, Q. Wang, D. Wang, J. Yang, P. Liu, T. Xu, Q. Yan, J. Zhang, K. Zen and C. Y. Zhang.** Secreted monocytic miR-150 enhances targeted endothelial cell migration. *Mol Cell*. 2010; **39**(1): 133-144.

Table 1.

Top listed results of SAMcell

miRNA	Fold Change	P-value
miR-106b	0.90005	0.000251
miR-148b	0.901037	7.55E-05
miR-21	0.905	0.019
miR-135b	0.915	0.00039
miR-296-5p	0.916	0.00053
miR-590-5p	0.921	0.1019
miR-33a	0.923	0.029
Let-7f-1-3p	0.925	0.0498
miR-29c*	0.926	0.004
Let-7i	0.927	0.027
miR-204	0.9278	0.008
miR-221	0.931	0.121
miR-190	0.934	0.117
miR-7	0.935	0.058
miR-331-3p	0.936	0.046

Table 2.

miRNAs-Nox2 predicting binding sites from Targetscan database

	Predicted consequential pairing of target region (top) and miRNA (bottom)
Nox2 3'UTR	5' ...UCUAUGGUUUUGAGAGCACUUUU...
	| | | | | | |
Has-miR-106b	3' UAGACGUGACAGUCGUGAAAU
Nox2 3'UTR	5' ...CCCAGAAUCCUCAGGGCACUGAG...
	| | | | | |
Has-miR-148b	3' UGUUUCAAGACAUCACGUGACU
Nox2 3'UTR	5' ...UCAAUUUUAGAAUCAAAAGGGAA...
	| | | | | | |
Has-miR-204	3' UCCGUAUCCUACUGUUUCCCUU
Nox2 3'UTR	5' ...AAAAUAAAAAAGGCAAAAGGGAG...
	| | | | | | |
Has-miR-204	3' UCCGUAUCCUACUGUUUCCCUU

Figure 1.Schematic diagram of the screening strategy to identify miRNAs targeting human Nox2. miRNA mimics were printed on the self-assembled cell microarray together with the transfection reagent. Hela cells stably expressing enhanced green fluorescent protein (eGFP) fused with the 3'UTR from human Nox2 were seeded on the array. Human Nox2 siRNA was used as positive control (PC) and scrambled miRNA was used as negative control (NC). In total, 266 miRNAs with conserved sequences between humans and mice were screened. After bioinformatics analysis and validation, three miRNAs were chosen for further study.

Figure 2.miRNAs regulated both humans and mice Nox2 expression. A and **B,** Relative luciferase activity in Hela cells transfected with indicated miRNAs or control vector with human (**A**) and mouse (**B**) Nox2 3'UTR driven reporter constructs, n=5. Shaded bars in **A** show 3';UTR with mutated predicted binding sites (Targetscan). **C** and **D,** Real-time PCR for Nox2 in PMA induced THP-1 (**C**) and RAW 264.7 (**D**) cells 48 hours after transfection with indicated miRNA or control vector. GAPDH was used as the loading control, n=3. **E** and **F,** Immunoblots for Nox2 in PMA induced THP-1 (**E**) and RAW 264.7 (**F**) cells 48 hours after transfected with indicated miRNAs or control vector. GAPDH was used as the loading control. **p<0.01, ***p<0.001 (t-test).

Figure 3.miRNAs inhibited superoxide production in humans and mice macrophages. A, Superoxide production levels in THP-1 (upper) and RAW 264.7 (bottom) cells were detected with ROSstar dye staining after stimulated by PMA and transfected with indicated miRNAs or control vector, n=3. Scar bar = 100 μm. **B** and **C,** Quantification of superoxide production levels in THP-1 (**B**) and RAW 264.7 (**C**) cells by comparing fluorescence intensity of indicated group. **D** and **E,** Representativeimages (**D**) and quantification (**E**) of superoxide production levels in RAW 264.7 when Nox2 was over expressed together with miRNAs transfection, n=3.*p<0.05,***p<0.001 (t-test).

Figure 4. Comparison of miRNAs mix and single miRNA function and inhibition on pro-inflammatory related genes. A, Real-time PCR for Nox2 mRNA in RAW 264.7 after transfection with indicated miRNA or a mixture of all 3 miRNAs normalized to miR-106b treatment. Data show no difference between individual miRNAs or combinations, n=3. **B,** Quantification of relative fluorescence intensity with DHE staining in RAW 264.7 after transfection with indicated miRNA, result of miR-106b used as control. No significant difference among four groups, n=3.**C-E,** Real-time PCR for IL-1β (**D**), IL-6 (**E**), and TNF-α (**F**) mRNA in RAW 264.7 after transfection with indicated miRNA. **F-H,** ELISA assay for IL-1β (**F**), IL-6 (**G**), and TNF-α (**H**) protein level in RAW 264.7, n=3.*p<0.05, **p<0.01, ***p<0.001 (t-test).

Figure 5.PK3-miRNAs nanoparticles redued Nox2 expression and activity in RAW 264.7 cells. A, Fold change of miRNAs levels in RAW 264.7 cells after treated with indicated PK3-miRNAs nanoparticles by real-time PCR. U6 was used as the loading control, n=3. **B,** Real-time PCR of Nox2 in RAW 264.7 cells after treatment with indicated PK3-miRNA or control nanoparticles. GAPDH was used as the loading control, n=3. **C** and **D,** Representative images (**C**) and quantification (**D**) of superoxide production levels in RAW 264.7 cells treated with indicated nanoparticles by ROSstar dye, n=3. ***p<0.001 (t-test).

Figure 6.PK3-miRNAs nanoparticles inhibited Nox2 expression and activity in vivo.A and **B,** Representative images (**A**) and quantification (**B**) of Nox2 (red) levels by in situ immunostaining on frozen sections from indicated mouse heart tissues. Cell nuclei were stained by Hoechst (blue), n=5.Scar bar = 100 μm. **C** and **D,** Representative images (**C**) and quantification (**D**) of superoxide production levels by DHE staining on frozen sections from indicated mouse heart tissues. Cell nuclei were stained by Hoechst, n=5. Scar bar = 100 μm. **p<0.01; ***p<0.001 (One-way ANOVA followed by Bonferroni post-test). **E,** Representative images of Nox2 (red), CD68 (green) and cell nuclei (blue) by in situ immunostaining on frozen sections.

Figure 7. PK3-miRNA nanoparticles improved cardiac function after MI. A, Echocardiographic pictures of mice 3 days after indicated treatment. **B and C,** Echocardiographic parameters fractional shortening (**B**) and ejection fraction (**C**) from indicated group of mice,n=5. **p<0.01; ***p<0.001 (One-way ANOVA followed by Bonferroni post-test).**D and E,** Representative images (D) and grouped data (E) from infarct size experiments, n>4. **p<0.01, ***p<0.001 (One-way ANOVA followed by Bonferroni post-test).

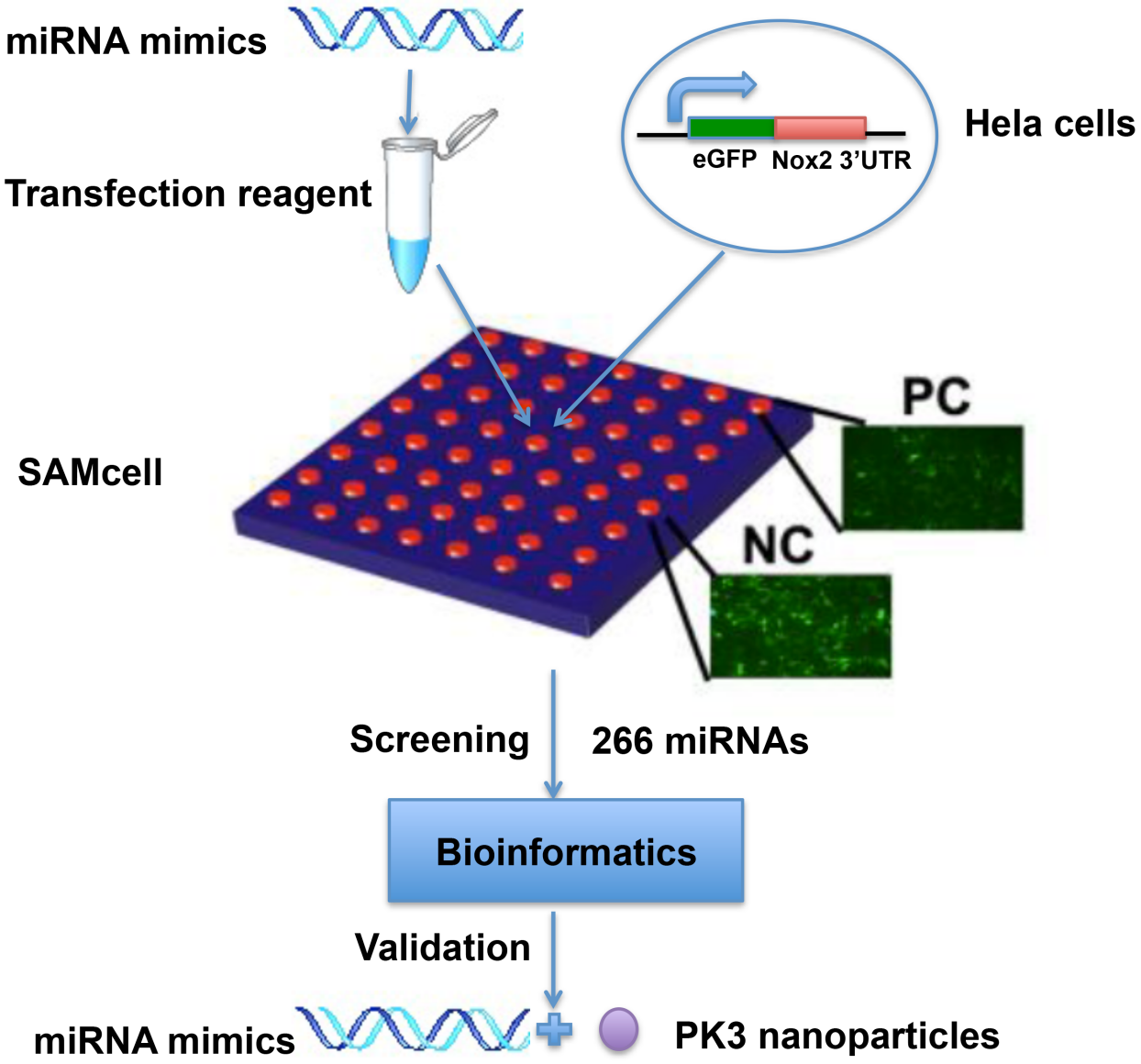
miRNA mimics
Transfection reagent
eGFP Nox2 3'UTR
Hela cells
SAMcell
PC
NC
Screening
266 miRNAs
Bioinformatics
Validation
miRNA mimics
PK3 nanoparticles

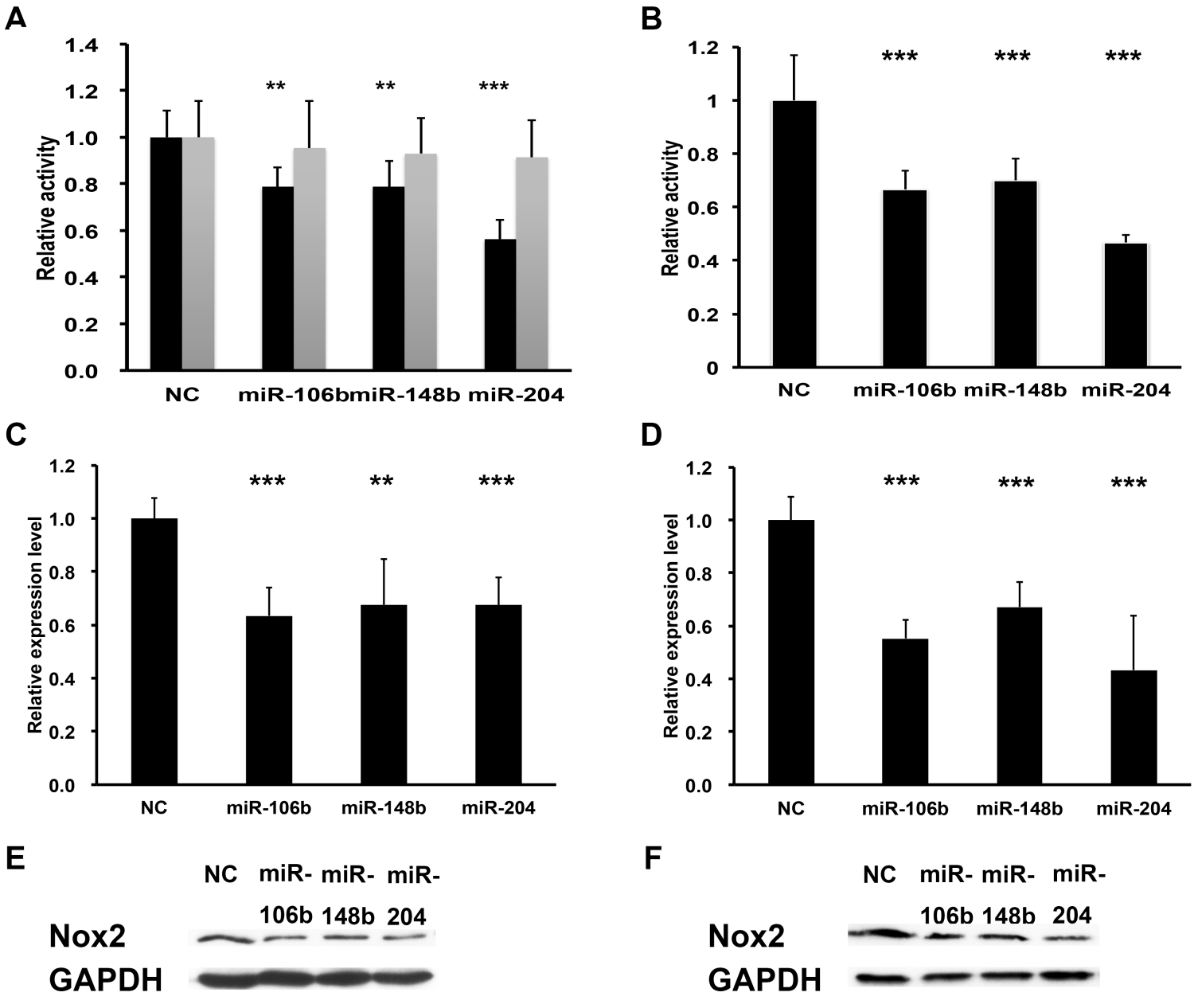
A
Relative activity
1.4
1.2
1.0
0.8
0.6
0.4
0.2
0.0
**
**
***
NC
miR-106b
miR-148b
miR-204
B
Relative activity
1.2
1
0.8
0.6
0.4
0.2
0
***
***
***
NC
miR-106b
miR-148b
miR-204
C
Relative expression level
1.2
1.0
0.8
0.6
0.4
0.2
0.0
***
**
***
NC
miR-106b
miR-148b
miR-204
D
Relative expression level
1.2
1.0
0.8
0.6
0.4
0.2
0.0
***
***
***
NC
miR-106b
miR-148b
miR-204
E
NC
miR-106b
miR-148b
miR-204
Nox2
GAPDH
F
NC
miR-106b
miR-148b
miR-204
Nox2
GAPDH

A

PMA Treatment

Blank | NC | miR-106b | miR-148b | miR-204

THP-1

RAW 264.7

B

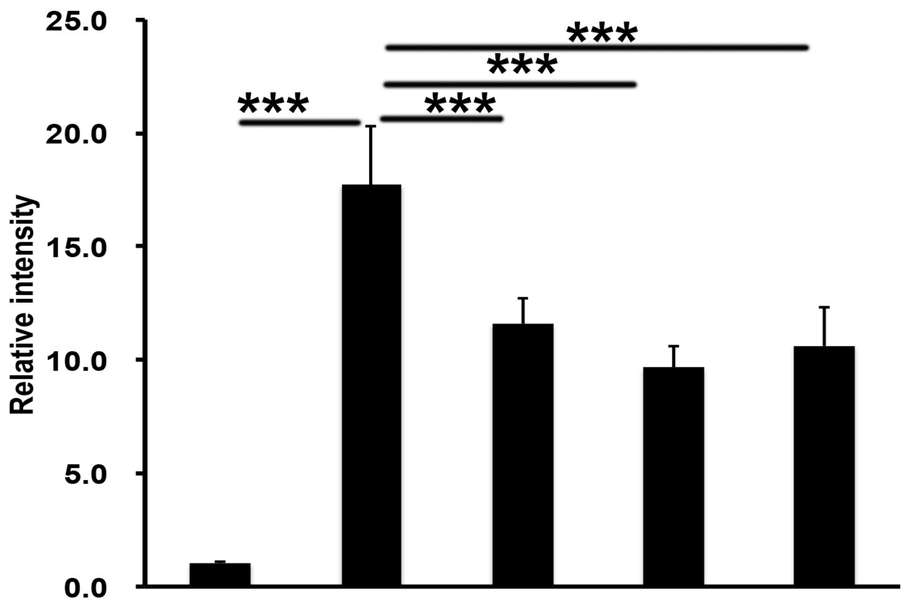

C

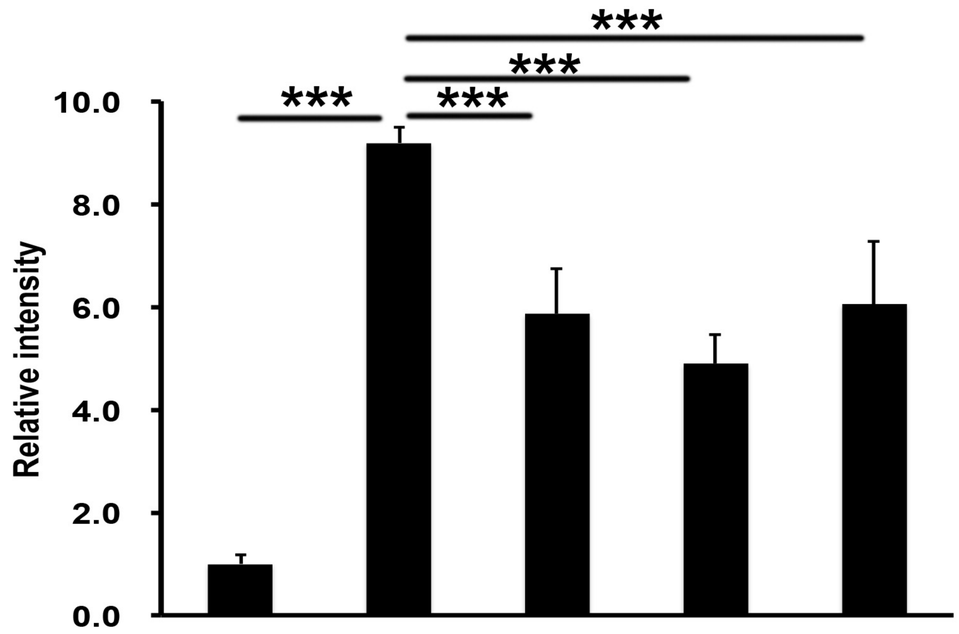

D

PMA Treatment

Blank | NC | miR-106b | miR-148b | miR-204

Nox2 Over-expression

E

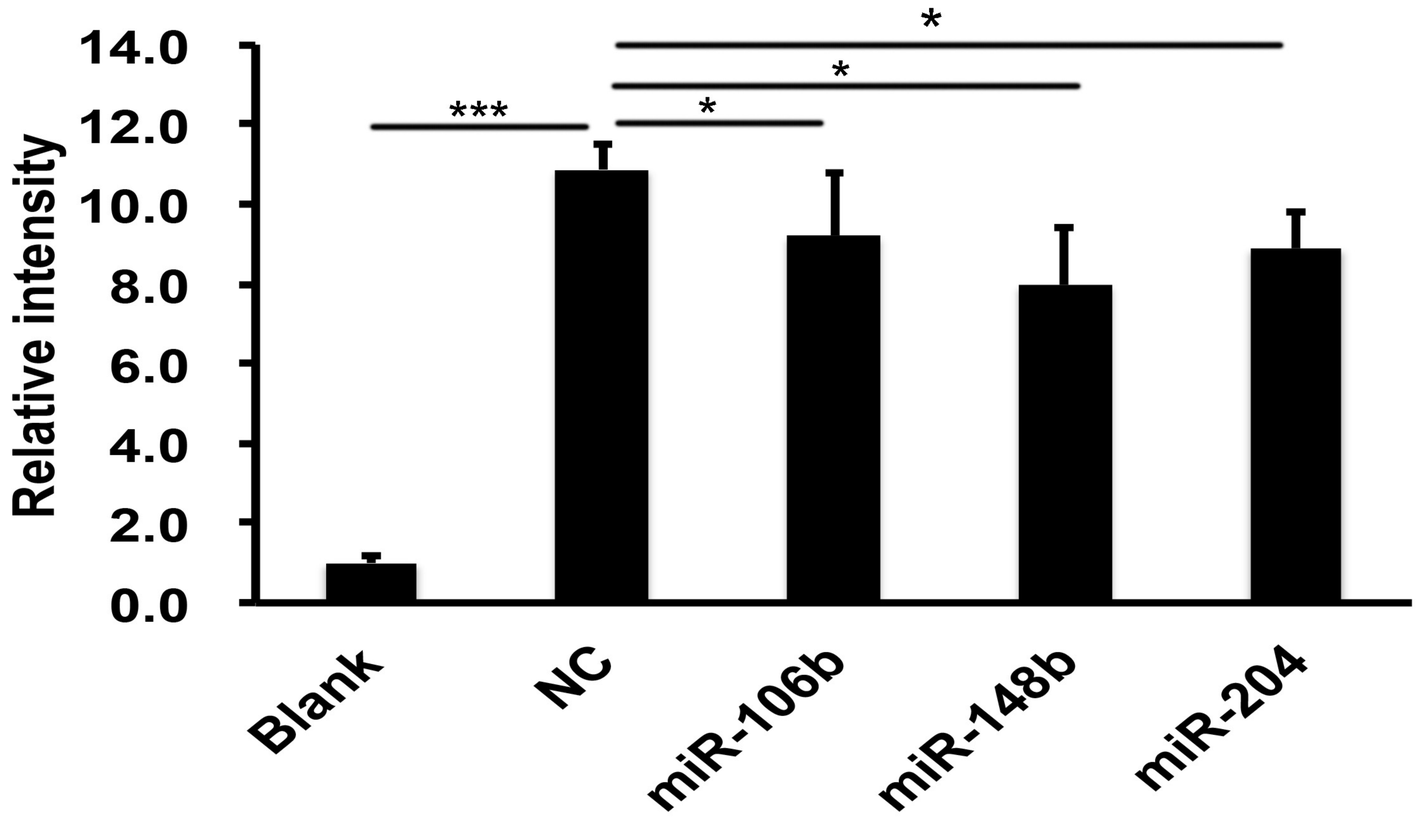

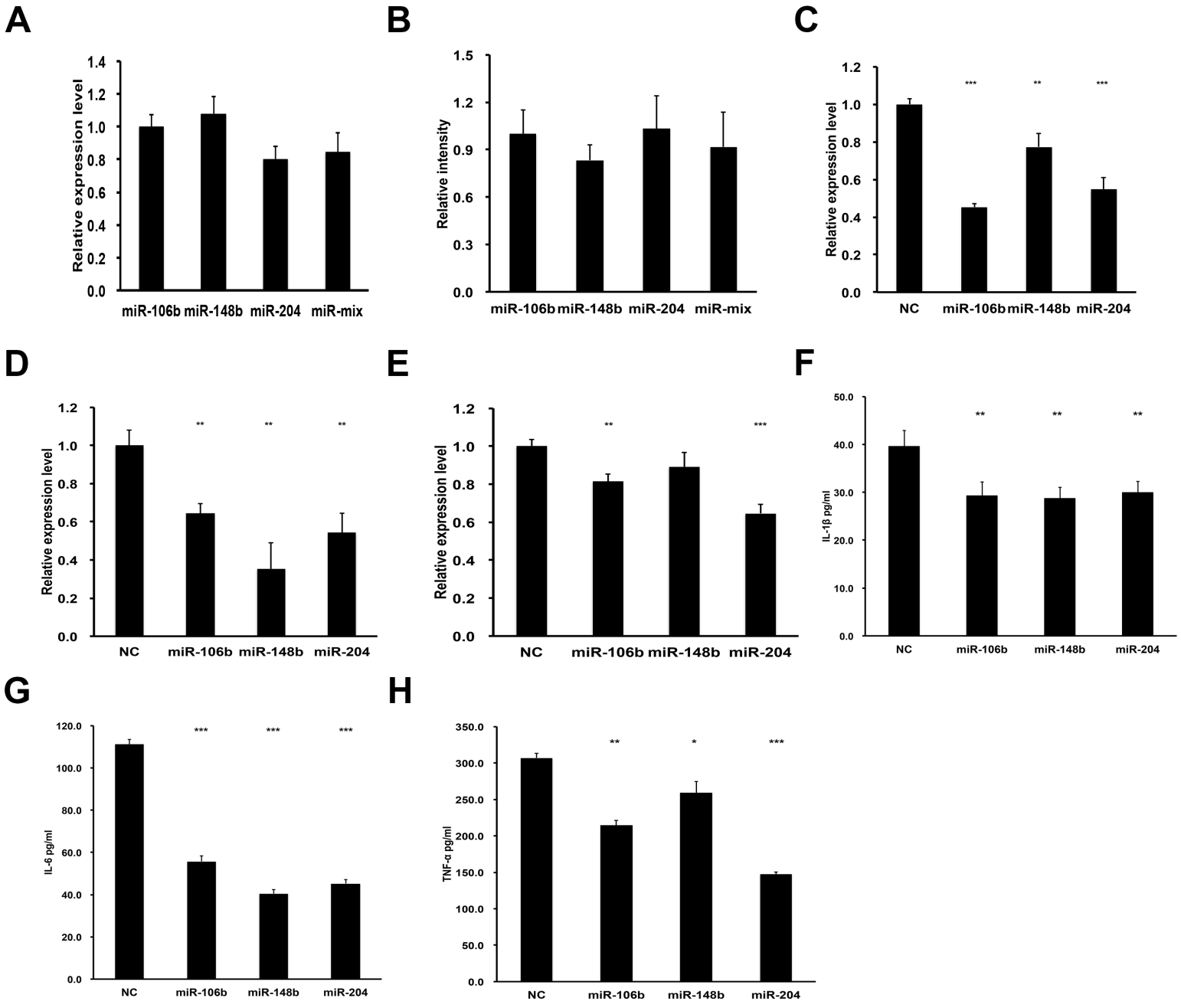
A
Relative expression level
1.4
1.2
1.0
0.8
0.6
0.4
0.2
0.0
miR-106b miR-148b miR-204 miR-mix
B
Relative intensity
1.5
1.2
0.9
0.6
0.3
0.0
miR-106b miR-148b miR-204 miR-mix
C
Relative expression level
1.2
1.0
0.8
0.6
0.4
0.2
0.0
***
**
***
NC miR-106b miR-148b miR-204
D
Relative expression level
1.2
1.0
0.8
0.6
0.4
0.2
0.0
**
**
**
NC miR-106b miR-148b miR-204
E
Relative expression level
1.2
1.0
0.8
0.6
0.4
0.2
0.0
**
***
NC miR-106b miR-148b miR-204
F
IL-1β pg/ml
50.0
40.0
30.0
20.0
10.0
0.0
**
**
**
NC miR-106b miR-148b miR-204
G
IL-6 pg/ml
120.0
100.0
80.0
60.0
40.0
20.0
0.0
***
***
***
NC miR-106b miR-148b miR-204
H
TNF-α pg/ml
350.0
300.0
250.0
200.0
150.0
100.0
50.0
0.0
**
*
***
NC miR-106b miR-148b miR-204

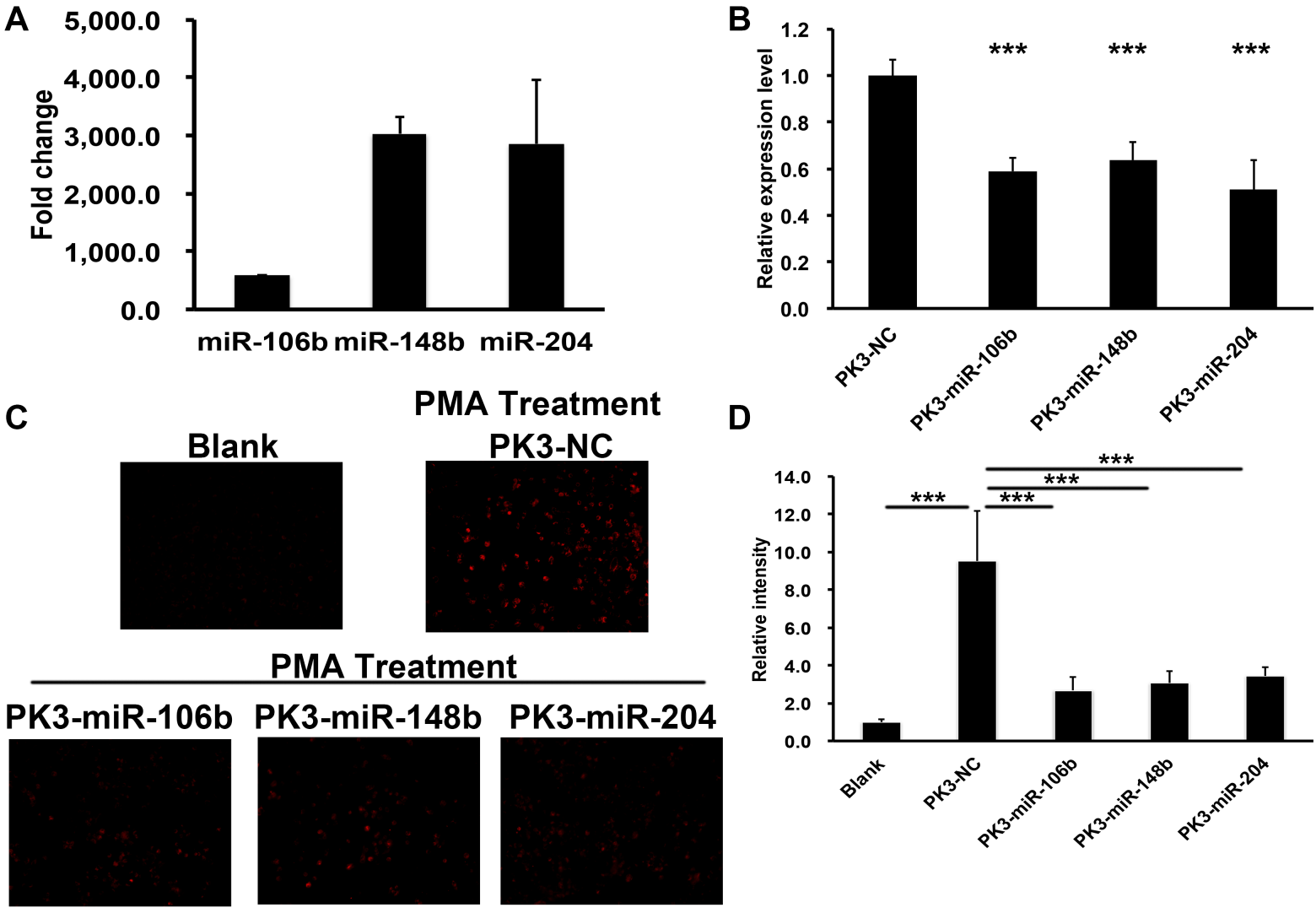
A
5,000.0
4,000.0
3,000.0
2,000.0
1,000.0
0.0
Fold change
miR-106b
miR-148b
miR-204
B
1.2
1.0
0.8
0.6
0.4
0.2
0.0
Relative expression level
***
***
***
PK3-NC
PK3-miR-106b
PK3-miR-148b
PK3-miR-204
C
Blank
PMA Treatment
PK3-NC
PMA Treatment
PK3-miR-106b
PK3-miR-148b
PK3-miR-204
D
14.0
12.0
10.0
8.0
6.0
4.0
2.0
0.0
Relative intensity
***
***
***
***
Blank
PK3-NC
PK3-miR-106b
PK3-miR-148b
PK3-miR-204

A

Sham Surgery

MI Surgery

Blank

PK3-NC

PK3-miR-106b

PK3-miR-148b

PK3-miR-204

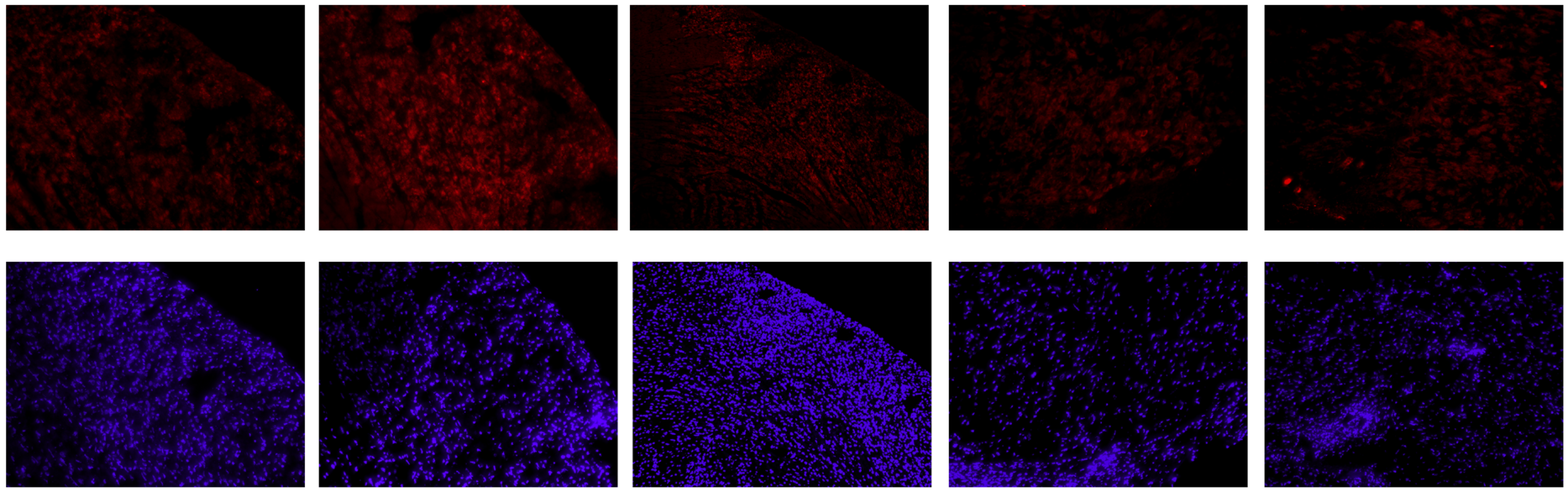

B

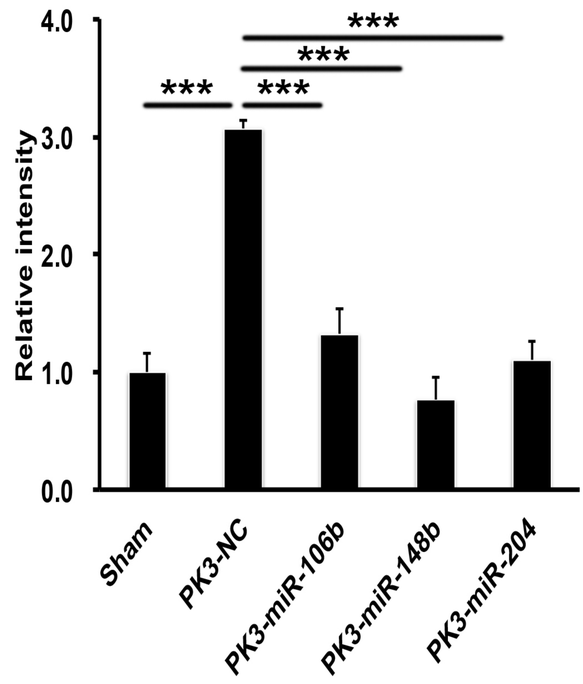

C

Sham Surgery

MI Surgery

Blank

PK3-NC

PK3-miR-106b

PK3-miR-148b

PK3-miR-204

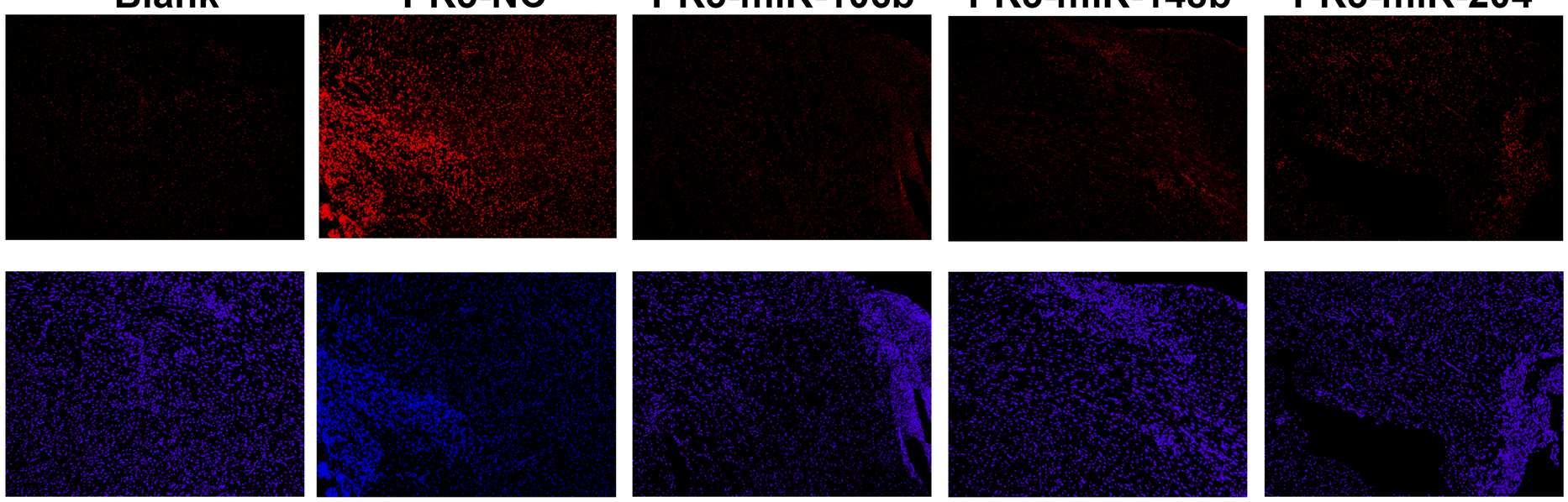

D

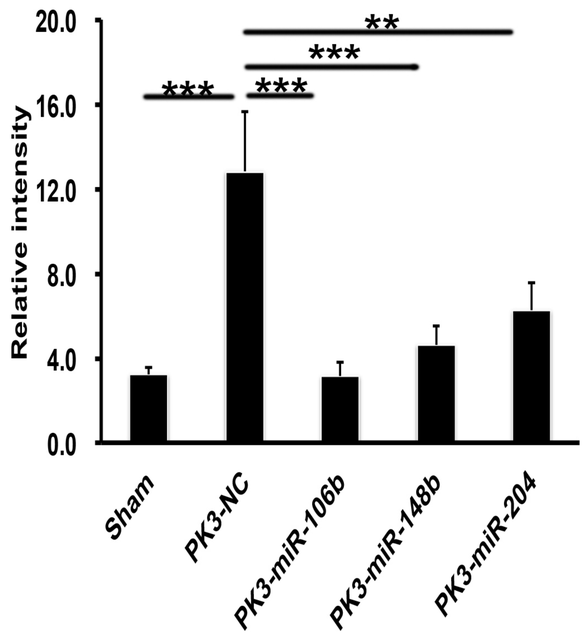

E

PK3-NC

PK3-miR-106b

PK3-miR-148b

PK3-miR-204

DAPI

Nox2

CD68

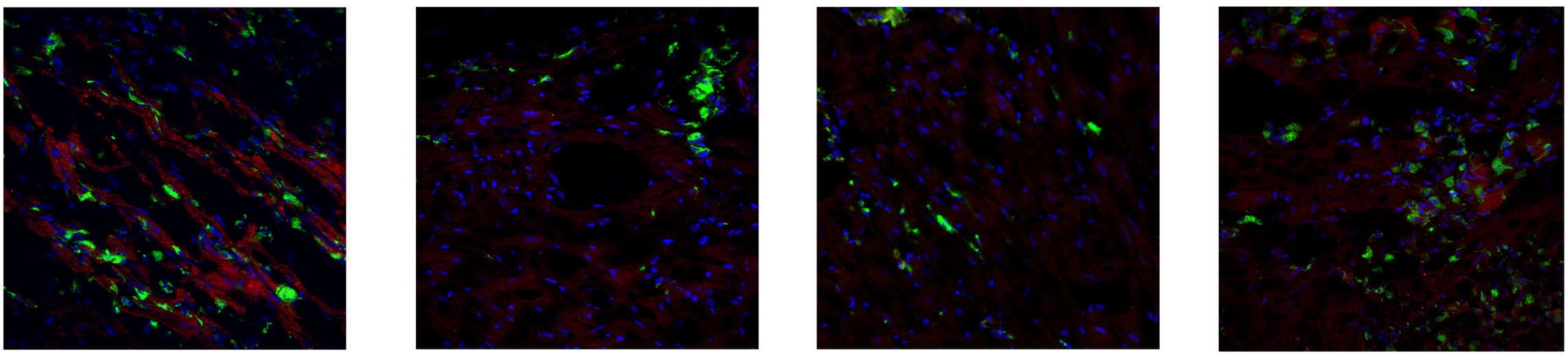

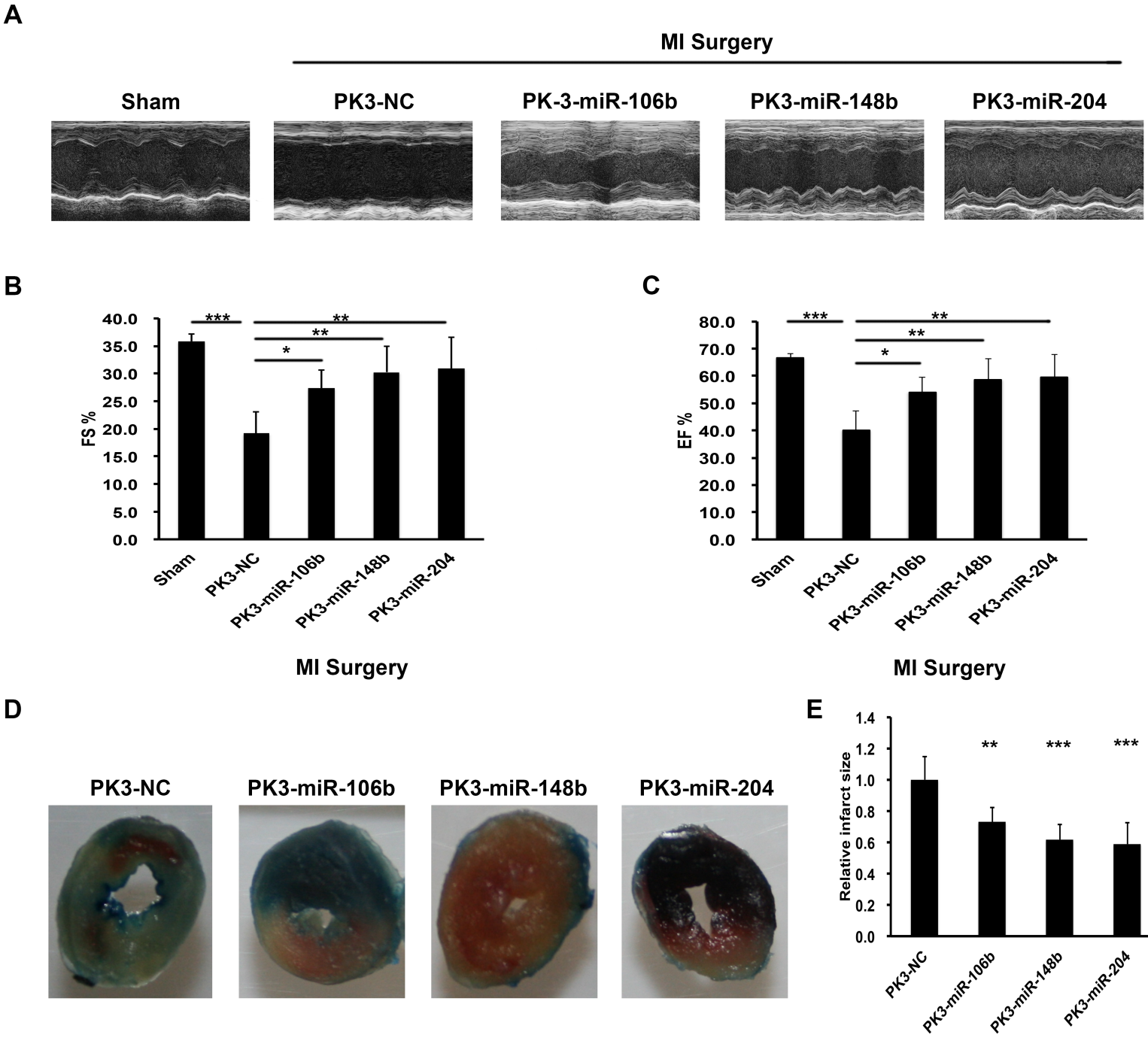
A
MI Surgery
Sham
PK3-NC
PK-3-miR-106b
PK3-miR-148b
PK3-miR-204
B
FS %
40.0
35.0
30.0
25.0
20.0
15.0
10.0
5.0
0.0
***
**
**
*
Sham
PK3-NC
PK3-miR-106b
PK3-miR-148b
PK3-miR-204
MI Surgery
C
EF %
80.0
70.0
60.0
50.0
40.0
30.0
20.0
10.0
0.0
***
**
**
*
Sham
PK3-NC
PK3-miR-106b
PK3-miR-148b
PK3-miR-204
MI Surgery
D
PK3-NC
PK3-miR-106b
PK3-miR-148b
PK3-miR-204
E
Relative infarct size
1.4
1.2
1.0
0.8
0.6
0.4
0.2
0.0
**
***
***
PK3-NC
PK3-miR-106b
PK3-miR-148b
PK3-miR-204